LA-UR- 09-06178

Approved for public release; distribution is unlimited.

Title:	Meltwater flux and runoff modeling in the ablation area of jakobshavn Isbrae, West Greenland
Author(s):	Sebastian H. Mernild, LANL; Glen Liston, Colorado State University; Konrad Steffen, University of Colorado; and Petr Chylek. LANL.
Intended for:	Journal of Glaciology

Los Alamos
NATIONAL LABORATORY
EST. 1943

Form 836 (7/06)

Meltwater flux and runoff modeling in the ablation area of Jakobshavn Isbræ, West Greenland

SEBASTIAN H. MERNILD

Climate, Ocean, and Sea Ice Modeling Group, Computational Physics and Methods, Los Alamos National Laboratory, New Mexico, USA, and International Arctic Research Center and Water & Environmental Research Center, University f Alaska Fairbanks, Alaska, USA

GLEN E. LISTON

Cooperative Institute for Research in the Atmosphere, Colorado State University, Colorado, USA

KONRAD STEFFEN

Cooperative Institute for Research in the Environmental Sciences, University of Colorado, Boulder, Colorado, USA

PETR CHYLEK

Los Alamos National Laboratory, Space and Remote Sensing Sciences, Los Alamos, New Mexico, USA

Submitted 8 April 2009 to Journal of Glaciology

Re-submitted 15 July 2009

Corresponding author address:

Dr. Sebastian H. Mernild

Climate, Ocean, and Sea Ice Modeling Group, Computational Physics and Methods (CCS-2)

Los Alamos National Laboratory,

Los Alamos, New Mexico 87545

USA

E-mail: mernild@lanl.gov

Abstract

The temporal variability in surface snow and glacier melt flux and runoff were investigated for the ablation area of Jakobshavn Isbræ, West Greenland. High-resolution meteorological observations both on and outside the Greenland Ice Sheet (GrIS) were used as model input. Realistic descriptions of snow accumulation, snow and glacier-ice melt, and runoff are essential to understand trends in ice sheet surface properties and processes. SnowModel, a physically based, spatially distributed meteorological and snow-evolution modeling system was used to simulate the temporal variability of Jakobshavn Isbræ accumulation and ablation processes for 2000/01–2006/07. Winter snow-depth observations and MODIS satellite-derived summer melt observations were used for model validation of accumulation and ablation. Simulations agreed well with observed values. Simulated annual surface melt varied from as low as 3.83×10^9 m^3 (2001/02) to as high as 8.64×10^9 m^3 (2004/05). Modeled surface melt occurred at elevations reaching 1,870 m a.s.l. for 2004/05, while the equilibrium line altitude (ELA) fluctuated from 990 to 1,210 m a.s.l. during the simulation period. The SnowModel meltwater retention and refreezing routines considerably reduce the amount of meltwater available as ice sheet runoff; without these routines the Jakobshavn surface runoff would be overestimated by an average of 80%. From September/October through May/June no runoff events were simulated. The modeled interannual runoff variability varied from 1.81×10^9 m^3 (2001/02) to 5.21×10^9 m^3 (2004/05), yielding a cumulative runoff at the Jakobshavn glacier terminus of ~2.25 m w.eq. to ~4.5 m w.eq., respectively. The average modeled Jakobshavn runoff of ~3.4 km^3 y^{-1} was merged with previous estimates of Jakobshavn ice discharge to quantify the freshwater flux to Illulissat Icefiord. For both runoff and ice discharge the average trends are similar, indicating increasing (insignificant) influx of freshwater to the Illulissat Icefiord for the period 2000/01–2006/07. This study suggests that surface runoff forms a minor part of the overall Jakobshavn freshwater flux to the fiord: around 7% (~3.4 km^3 y^{-1}) of the average annual freshwater flux of ~51.0 km^3 y^{-1} originates from the surface runoff.

KEY WORDS flux, Greenland Ice Sheet, Jakobshavn Isbræ, mass balance, melt extent, runoff, SnowModel

1. Introduction

The Greenland Ice Sheet (GrIS) is Northern Hemisphere's largest terrestrial permanent ice- and snow-covered area. The GrIS is a reservoir of water that is highly sensitive to changes in climate (e.g., Box et al. 2006, Fettweis 2007, Hanna et al. 2007, 2008, Mernild et al 2008). It is essential to assess the impact of climate change on the GrIS, since the temperature rise at higher northern latitudes is strongly correlated with global warming, and confirmed to increase at almost twice the global average rate in the past 100 years (IPCC 2007). Since 1957, Arctic air temperature increases have averaged more than 2°C (http://giss.nasa.gov/). A response to altered climate has already been observed on the GrIS, manifested by an accelerating surface melt extent, mass loss, and freshwater runoff, and thinning along the periphery (e.g., Krabill et al. 2000, 2004, Janssens and Huybrechts 2000, Zwally et al. 2002, Johannessen et al. 2005, Box et al. 2006, Fettweis 2007, Mernild et al. 2008, 2009a, Hanna et al. 2009). Also, at the local scale, e.g., in the Jakobshavn region, West Greenland, the same trend in melt extent and ice thinning are observed (e.g., Luckman and Murray 2005, Chylek et al. 2007).

Efforts to model the GrIS mass-balance, its dynamic processes, changes, and contribution to the global eustatic sea level rise, still suffer from important uncertainties and limitations (Parizek and Alley 2004, Lemke at al. 2007, Broeke et al. 2008). The mechanisms that link climate and ice dynamics are poorly understood, and current numerical ice sheet models do not simulate these changes realistically (Nick et al. 2009). Fortunately, modeling the GrIS surface mass-balance (SMB) is relatively well understood and documented in numerical models (e.g., Box et al. 2006, Fettweis 2007, Hanna et al. 2007, Mernild et al 2008). To estimate the impact of seasonally changing processes on the GrIS surface hydrological cycle, different seasonal processes need to be understood and accounted for. Throughout the GrIS, much of the winter precipitation falls as a solid under windy conditions. As winter progresses, the solid precipitation accumulates on the ground and is frequently redistributed during blowing snow events. A further consequence of this blowing snow is that significant portions (10–50%) of snow cover can be returned to the atmosphere by sublimation of windborne snow particles (e.g., Liston and Sturm 1998, Pomeroy and Essery 1999).

As spring and summer progress, the variation, duration, and intensity of snow and glacier melt increases in response to the impact in weather and climate (e.g., insolation, temperature inversions, and wind speed) and surface characteristics (e.g., albedo, roughness). The moisture in this system also changes phase (solid, liquid, and vapor) throughout the year as part of various physical processes and in response to the available surface and snowpack energy fluxes. The role of

snowpack meltwater retention is also important to account for; the overall GrIS runoff would be overestimated by approximately 20–30% if no model retention/refreezing routines were included in the model simulations (e.g., Hanna et al., 2002, 2005, 2008, Mernild et al. 2008). All of these seasonally changing processes directly impact the GrIS surface hydrological cycle's seasonal evolution (mass fluxes), including the influx of freshwater to the ocean and is subsequent role in controlling global eustatic sea level (e.g., Dowdeswell et al. 1997; ACIA 2005; IPCC 2007).

This study attempts to improve our quantitative understanding of the Jakobshavn Isbræ drainage area melt distributions and its surface water balance components, particularly changes in freshwater runoff and net mass-balance. The goal of this study was to apply a well-tested, state-of-the-art modeling system, SnowModel (Liston and Elder 2006a, Mernild et al. 2006, Liston et al. 2007), to the Jakobshavn region. SnowModel routines were compared to independent *in situ* field snow water equivalent (SWE) depth and satellite-derived melt extent observations. We performed model simulations for a 7-year period (2000/01 through 2006/07) with the following objectives: 1) to simulate winter processes related to snow accumulation, snow redistribution by wind, and snow sublimation for the Jakobshavn Isbræ drainage area; 2) to simulate summer snowmelt and glacier-ice melt for the drainage area; 3) to compare modeled outputs with available independent observational datasets; 4) to generate time series and area-distributed runoff fluxes from the seasonal snowpack and the exposed glacier surface to be used as meltwater inputs to hydrological models; 5) to compare the trends in simulated runoff with previous estimates of Jakobshavn ice discharge and merge simulate runoff with ice discharge to quantify the freshwater flux to Illulissat Icefiord; and 6) to model the net mass-balance and the annual variability of the equilibrium line altitude (ELA) location.

2. Study area

a. Physical settings, meteorological stations, and climate

The Jakobshavn Isbræ is located on the west coast of Greenland (69°N latitude; 49°W longitude) approximately 55 km east of the town Ilulissat (Jakobshavn) (Figure 1). The Isbræ is Greenland's largest outlet glacier and a prolific exporter of ice (~50 Gt y^{-1}; Rignot et al. 2008) into the fiord, draining approximately 6–7% of the GrIS by area (92.080 km^2) (e.g., Luckman and Marray 2005, Holland et al. 2008). Since the first observation in 1850, there has been an almost continuous recession of the Jakobshavn Isbræ of around 40 km through the E-W orientation Ilulissat Icefjord. The ice front has receded at a steady rate of about 0.3 km y^{-1} (1850–1964) (e.g., Weidick and

Bennike 2009), coming to rest approximately 15–18 km down stream from the present location until 2001. The ice front then began to recede again far more rapidly at about 3 km y^{-1} to the present location (http://svs.gsfc.nasa.gov/vis/a000000/a003300/ a003395/).

The simulated Ilulissat region (68,872 km^2) (Figure 1) includes the area of interest (12,750 km^2) (Figure 1a), covering the W-part of the GrIS, and the lower part (the ablation area) of the Jakobshavn Isbræ drainage area (5,340 km^2). The area of interest is characterized with elevations ranging up to 1,840 m a.s.l. The land cover is dominated by ice in the upper parts of the terrain, and ocean/fjord and bare bedrock/vegetation in the lower parts (Figures 1c and 1d).

Five meteorological stations are located within the simulation domain, and four of them within the area of interest (Figure 1d). Station Aasiaat (Egedesminde) (68°42′N, 52°45′W; 88 m a.s.l.; a standard synoptic Danish Meteorological Institute (DMI) WMO meteorological station) is located within the town of Aasiaat representative of the Disko Bay and fiord conditions. Station JAR3 (69°23′N, 50°18′W; 283 m a.s.l.), JAR2 (69°25′N, 50°03′W; 542 m a.s.l.), JAR1 (69°29′N, 49°41′W; 962 m a.s.l.), and Swiss Camp (69°34′N, 49°19′W; 1,140 m a.s.l.) are all part of the Greenland Climate Network (GC-Net) located on the ice sheet, and representative of the GrIS conditions (for further information about the GC-Net stations see Steffen (1995), Steffen and Box (2001)). Swiss Camp is located close to the W-GrIS ELA (the ELA is defined as the elevation where the net mass-balance is zero).

The Ilulissat region is considered to be Low Arctic according to Born and Böcher (2001). The mean annual air temperature for the region (2000–2007) is -7.2°C. Mean annual relative humidity is 83% and mean annual wind speed is 6.1 m s^{-1}. The corrected mean total annual precipitation (TAP) is 810 mm w.eq. y^{-1} (corrected after Allerup et al. 1998, 2000).

3. Water balance components

Throughout the year, different surface processes (snow accumulation, snow redistribution, blowing-snow sublimation, surface evaporation, and melting) on snow and glacier ice affect the surface glacier mass-balance and the high-latitude water balance, including runoff. The yearly water balance equation for a glacier can be described by:

$$P - (E+SU) - R \pm \Delta S = 0 \pm \eta \qquad (1)$$

where P is the precipitation input from snow and rain (and possible condensation), E is evaporation, SU is sublimation (including blowing-snow sublimation), R is runoff, and ΔS is change in storage (ΔS is also referred as the SMB (surface mass-balance)) from changes in glacier storage and snowpack storage. Glacier storage also includes changes in supraglacial storage (lakes, pond, channels, etc.), englacier storage (ponds and the water table), and subglacier storage (cavities and lakes); glacier storage components were not accounted for in this study. Here, η is the water balance discrepancy (error). The error term should be 0 (or small) if the major components (P, E, SU, R, and, ΔS) have been determined accurately. Here, a change in storage is calculated by the residual value.

4. SnowModel

a. SnowModel description

SnowModel (Liston and Elder 2006a) is a spatially distributed meteorological and snowpack evolution modeling system. It is made up of five submodels: MicroMet (a quasi–physically based meteorological distribution model) defines the meteorological forcing conditions (Liston and Elder 2006b); EnBal calculates the surface energy exchanges, including melt (Liston 1995, Liston et al. 1999); SnowPack simulates heat and mass transfer processes, and snow depth and water equivalent evolution (Liston and Hall 1995); and SnowTran-3D is a blowing-snow model that accounts for snow redistribution by wind (Liston and Sturm 1998, 2002; Liston et al. 2007). SnowModel also includes a snow data assimilation submodel (SnowAssim; Liston and Hiemstra 2008) that can be used to assimilate available snow measurements to create simulated snow distributions that closely match observed distributions when and where they occur (Liston et al. 2008). SnowModel was originally developed for glacier-free landscapes. For glacier SMB studies in Arctic coastal regions, SnowModel was modified to simulate: 1) the glacier-ice melt after winter snow accumulation had ablated (Mernild et al. 2006, 2007); and 2) the influence of air temperature inversions on snowmelt and glacier mass-balance simulations where radiosonde data are present (Mernild and Liston 2009). For this study routines for temperature inversion were not included due to the lack of available radiosonde data in the area. SnowModel has been used over a wide variety of snow and glacier landscapes in the United States, Norway, East Greenland, the Greenland Ice Sheet and near-coastal Antarctica.

b. SnowModel input

To solve this system of equations, SnowModel requires spatially distributed fields of topography and land-cover, and temporally distributed point meteorological data (air temperature, relative humidity, wind speed, wind direction, and precipitation) obtained from meteorological stations located within the simulation domain. For this study, high-resolution data are obtained from five meteorological stations: four stations (JAR1 through JAR3, and Swiss Camp) from the GC-Net, and one standard synoptic DMI WMO operated station (Aassiat) (Figure 1 and Table 1).

Mean monthly lapse rates (1997–2005) based on air temperature observations from the transect between JAR1, JAR2, and JAR3 was used as model input (Table 2). The minimum monthly temperature lapse rate of -10.0°C km^{-1} occurred in October, and the maximum of -4.9°C km^{-1} occurred in June. The mean annual Jakobshavn lapse rate of -7.1°C km^{-1} is in line with the average western GrIS lapse rates of -7.8°C km^{-1} (Steffen and Box 2001), and the average GrIS values of -7.5°C km^{-1} (Mernild et al. 2008).

Across the Arctic, it is well-known that precipitation gauges significantly underestimate solid precipitation because of aerodynamic errors at the gauging station; especially under windy and cold conditions (e.g., Yang et al. 1999). Solid and liquid precipitation measurements at the DMI meteorological station (Figure 1 and Table 2) were calculated from Helman–Nipher shield observations corrected according to Allerup et al. (1998, 2000) and used as input for SnowModel. Solid (snow) precipitation for JAR 1–3 was calculated from snow-depth sounder observations after the sounder data noise was removed and further used in SnowModel; these data are assumed to be accurate within ±10–15% (for further information about the precipitation calculations see Mernild et al. 2007, 2008).

The simulations span the 7-year period 1 September 2000 through 31 August 2007.Simulations were performed using a one-day time step, although snow- and ice-melt, and blowing snow, are threshold processes that may not be accurately represented by this time step. Therefore, daily simulated melt and blowing-snow processes were compared against hourly simulated values from a test area, the Mittivakkat Glacier (31 km^2), SE Greenland (Mernild and Liston 2009). Glacier winter, summer, and net mass-balances significantly ($p<0.01$; where p is the level of significance) differed 2%, 3%, and 8%, respectively. We also recognize that daily-averaged atmospheric forcing variables, in contrast to hourly data, smoothed the meteorological driving data.

Greenland topographic data for the model simulations were provided by Bamber et al. (2001), and the image-derived correction by Scambos and Haran (2002). For the model simulations, this DEM was aggregated to a 500 m grid-cell increment and clipped to yield a 343.5 by 200.5 km

simulation domain (the Ilulissat region) (Figure 1). The domain includes the area of interest (127.0 by 100.0 km) that encompassed the Jakobshavn Isbræ area (Figure 1d). The Jakobshavn Isbræ ice front was confirmed or estimated for each year according to position illustrated on the satellite image ([http://svs.gsfc.nasa.gov/vis/a000000/a003300/a003395/]). SnowModel is a surface model producing first-order effects of climate change; it does not include glacio-hydro-dynamic and glacio-sliding routines. Therefore, using a time-invariant DEM will yield melt uncertainties in areas where the GrIS surface elevation is modified by the arrival of relatively warm subsurface ocean water (Holland et al. 2008) and by GrIS dynamic processes. Between 1997 and 2001 e.g., NASAs Airborne Topographic Mapper surveys showed an approximately 35 m reduction in surface elevation on the floating ice tongue (Holland et al. 2008). Observations from laser-altimeter surveys along tracks on Jakobshavn Isbræ show dynamic thinning with rates of up to 10 m y^{-1} between 1997 and 2003 (Krabill et al. 2004). The dynamic thinning continues, with increasing rates and with the thinning zone migrating inland as shown from the repeat survey between 2002 and 2006 (Joughin et al. 2008). In the simulations presented herein, the dynamic thinning are assumed to be second-order processes and not accounted for.

Each grid cell within the domains was assigned a USGS Land Use/Land Cover System class according to the North American Land Cover Characteristics Database (e.g., Mernild et al. 2008). The snow-holding depth (the snow depth that must be exceeded before snow can be transported by wind) was assumed to be constant. The snow albedo is calculated using Douville et al. (1995) and Strack et al. (2004), gradually decreasing the albedo from 0.8 to a minimum of 0.5 as the snow ages. The albedo is reset to 0.8 after 0.003 mm SWE has fallen. When the snow is ablated, the GrIS surface ice conditions are used. Albedo was assumed to be 0.4 for ice; however, the GrIS ablation area is characterized by lower albedo on the margin and an increase in albedo toward the ELA, where a veneer of ice and snow dominate the surface (Boggild et al. 2006). The emergence and melting of old ice in the ablation area creates surface layers of dust (black carbon particles) that were originally deposited with snowfall higher on the ice sheet. This debris cover is often augmented by locally-derived windblown sediment. Particles on or melting into the ice change the area-average albedo, increasing melt. User-defined constants for SnowModel are shown in Table 3 (for parameter definitions see Liston and Sturm 1998, 2002).

c. SnowModel calibration, validation, and uncertainty

SnowModel was chosen for this study because of its robustness and ease of implementation over new simulation domains. This model demands rather limited input data, an important consideration in areas like Jakobshavn, for which data are sparse due to rough terrain, harsh climatic conditions, and its remote location. To assess the general performance of SnowModel simulated distributed meteorological data, snow-evolution, snow and ice surface melt, glacier net mass-balance, and other snow and ice processes, simulated values were tested against independent observations. First, SnowModel/MicroMet distributed meteorological data were compared against independent Greenland meteorological station data both on and outside the GrIS, indicating respectable (84–87% variance for air temperature, 49–55% for wind speed, 49–69% for precipitation, and 48–63% for relative humidity) representations of meteorological conditions (for further information see Mernild et al. 2008, Mernild and Liston 2009). Second, few validation observations for *in-situ* snow-evolution, snow and ice surface melt, and glacier net mass-balance are available in Greenland. Therefore, SnowModel accumulation and ablation routines were tested qualitatively (by visual inspection) and quantitatively (cumulative values and linear regression) using independent *in-situ* observations on snow pit depths; glacier winter, summer, and net mass-balances; depletion curves; photographic time lapses; and satellite images also from in and outside the GrIS (e.g., Mernild et al. 2006, 2009b, Mernild and Liston 2009). A comparison performed between simulated and observed values indicates a 7% maximum difference between modeled and observed snow depths, glacier mass-balance, and snow cover extent.

To assess the winter and summer model performance for this Jakobshavn study the simulated end-of-winter SWE depth and the summer melt extent were compared with Swiss Camp SWE depth and Moderate Resolution Imaging Spectroradiometer (MODIS) satellite-derived melt extent observations, respectively. Swiss Camp SWE depth was measured as an average of ten different measurements at the beginning of May, and used to validate and adjust the SnowModel simulated SWE depth. The simulated SWE was underestimated in average by 13% (155 mm w.eq.), and up to 42% (430 mm w.eq.) for 2003/04 (Table 4). The iterative precipitation adjustment routines (for further information see Mernild et al. 2006 and SnowAssim: Liston and Hiemstra 2008), yield a simulated Swiss Camp SWE depth on 10 May that was within 1% of the observed SWE depth. The MODIS satellite-derived melt extent (the discrimination between dry and wet snow found by reflected visible and near-infrared radiation) was observed for two days: 7 July 2002 and 20 July 2005 based on a spatial resolution of 1.0 km^2 (Chylek et al. 2007). The criterion for MODIS-derived snow melt was a snow grain water thickness greater than 40 μm. The upper part of the Jakobshavn

drainage area is the area where the melting threshold of the algorithm did not show any melt. Satellite-derived and simulated average and standard deviated surface melt discrepancy between melt and non-melt boundaries is 7.8(±5.1) km; however the discrepancy can be up to ~22 km (Figure 3a). The difference in boundaries indicates a difference in melt area of ~10% and in surface melt of ~5% within the Jakobshavn Isbræ drainage area. It appears that our choice of a simple methodology provided estimates of the Jakobshavn surface melt distribution and related water balance components agree well with observed values. Nevertheless, it is important to keep in mind the limitation for SnowModel results when: 1) tested against sparse observations; and 2) when model uncertainties are largely determined by processes not yet represented by standard routines in the modeling system: e.g., routines for simulating changes in glacier area, size, and surface elevation according to glacier dynamic and sliding processes. Further, all ocean and fjord areas within the domain were excluded from model simulations. Also, changes in glacier storage based on supraglacial storage, englacial storage, subglacial storage, melt water routing, and evolution of the runoff drainage system are not calculated in SnowModel, even though they certainly have some influence on runoff magnitudes.

5. Results and discussion

Table 4 shows beginning-of-May observed and modeled SWE depth variations from Swiss Camp. Defined by our precipitation adjustment scheme for Swiss Camp (Mernild et al. 2006), the area of interest average SWE depth on 10 May varied from 440 mm w.eq. (2002/03; the year with the lowest SWE depth) to 2,020 mm w.eq. (2004/05; the year with greatest SWE depth), averaging 1,340(±480) mm w.eq. For the assumed end-of-winter (31 May; recognized as the end of the accumulation period) the SWE depth showed an almost similar average depth of 440 mm w.eq. for 2002/03 and 2,050 mm w.eq. for 2004/05 (See arrows on Figure 2a), averaging 1,370(±490) mm w.eq. In Figure 2a, the assumed end-of winter is marked by an arrow illustrating that this does not necessarily correspond to the maximum simulated average SWE depth (simulated end of winter), with a maximum difference of 7 days, and a difference of average SWE depth <9 mm w.eq. The average modeled SWE depth variation for the Jakobshavn drainage area is illustrated in Figure 2a for 2002/03 and 2004/05, indicating an increasing SWE depth throughout the accumulation period (September to May), a decreasing average SWE depth throughout the ablation period (June to August), and an end-of-year net accumulation in SWE depth (Figure 2a). Here, ablation includes phase-change processes like evaporation, sublimation, and melting. Within SnowModel, SnowTran-

3D simulates spatial snow deposition patterns in response to erosion and deposition, and EnBal calculates the energy flux available for snowmelt. For the end-of-year, SWE depth varied from 430 mm w.eq. (2002/03) to 1,040 mm w.eq. (2004/05); a surplus of SWE depth is located above the snow line (defined as the boundary between bare ice and snow cover). Our analysis of the spatial snow line distribution, in response to accumulation and ablation, showes an annual average maximum elevation between 928(±26) (2001/02) to 1,397(±11) (2000/01) (Figure 2d and Table 5). Our analysis of the spatial end-of-winter SWE depth distribution, in response to erosion and deposition (Figures 2b and 2c), shows an increasing accumulation from the GrIS margin to the higher inland elevations. This yielded an average SWE precipitation orographic effect for the Jakobshavn ablation area of 71(±16) mm w.eq. 100 m^{-1}, while the annual orographic increase was 83(±14) mm w.eq. 100 m^{-1}. These values are in line with gradients found in previous East Greenland studies on Ammassalik Island (65°N) by Mernild et al. (2006), and used in mountainous areas of Norway (Young et al. 2006).

Daily modeled time series of surface snow and glacier ice melt for 2001/02 (the year with the lowest cumulative melt) and 2004/05 (the year with the greatest cumulative melt) are illustrated in Figure 3b. For 2001/02 and 2004/05 the cumulative melt varied between 3.83 to 8.64×10^9 m^3, respectively, with maximum daily snow melt values of 2.26×10^8 m^3 and glacier ice of 1.39×10^8 m^3. In the early melt period (May and June), surface melt was mainly controlled by snowmelt, whereas later in the season (mid/end-of-July and August) when the snow cover was largely gone, surface melt was dominated by glacier-ice melt. When surface melting is defined by SnowModel, meltwater is assumed to run instantaneously when the surface consists of glacier ice. When a snow cover is present the SnowPack runoff routines take retention and internal refreezing into account when meltwater melts at the surface and penetrates through the snowpack. These routines do have a significant effect on the runoff lag time and the amount of runoff. Not including retention/refreezing routines in SnowModel would lead to a faster outflow of runoff and an overestimation of runoff to the ocean, and a consequent overestimation of the global sea level rise. If no retention/refreezing routines were included in SnowModel: 1) the initial seasonal runoff would occur between 23 to 85 days before; and 2) the Jakobshavn runoff would be overestimated between 65 to 110%, averaging 80%. This 80% value is above the previous values for the entire GrIS of approximately 25% estimated by Janssens and Huybrechts' (2000) single-layer snowpack model (used by e.g., Hanna et al. 2002; 2005; 2008), and of 19–27% by Mernild et al. 2008. The SnowPack sub-model in SnowModel is similar to the one used by Janssens and Huybrechts (2000); it does not calculate

vertical temperature changes through the snowpack. For the GrIS in total, the SnowModel retention and refreezing routines indicate that high runoff years are synchronous with low precipitation/accumulation years and vice versa. This trend was reported for the GrIS by Hanna et al. (2008) and Mernild et al. 2008, because higher volumes of meltwater were retained in the thicker snowpack, reducing runoff. This trend is most pronounced above the ELA where meltwater does not infiltrate far into the snowpack because of the snowpack's cold content – even during summer. For the Jakobshavn study the trend is opposite probably due to the direct energy contribution to the snowpack from precipitation, indicating insignificant increasing runoff with increasing precipitation (R^2=0.24; $p<0.25$).

Figure 4a illustrates the time series for the daily surface runoff production from both snow cover and glacier ice throughout winter and summer from 2001/02 through 2006/07, and Figure 4b presents the spatial distribution of cumulative runoff for 2001/02 (lowest annual cumulative runoff) and 2004/05 (highest cumulative runoff). The daily runoff values averaged 0.32×10^8 m^3, with a maximum daily value as high as 2.83×10^8 m^3, or 8.8 times the average runoff (Figure 4a). During winter (September/October through May/June), no runoff events where simulated. For 2000/01 through 2006/07 an exponential regression indicate a R^2-value (the explained variance) of 0.70 ($p<0.01$) between modeled daily runoff and mean daily air temperature; high temperatures correspond to high simulated runoff values. The first day for annual runoff varied almost a month from the beginning of May (day of year (DOY) 129) through beginning of June (DOY 159), averaging end-of-May (DOY 142) (Table 5). Then, a continuously modeled runoff period occurred until September/October, indicating the average number of runoff days to be 97(±17). In some areas of the Jakobshavn Isbræ (e.g., at the glacier terminus) as much as ~4.5 m w.eq. runoff was simulated for 2004/05, while only ~2.25 m w.eq occurred for 2001/02 (Figures 4b, 5a, and 5b). The amount of simulated runoff decreased with increasing altitude in average by 218 mm w.eq. 100 m^{-1} from the ice margin all the way to the runoff discrepancy between the runoff and non-runoff boundaries. The annual runoff boundary was located around 65 km from the Jakobshavn Isbræ and further inland, at 1,420 m a.s.l. to 1,870 m a.s.l., averaging 1,600(±170) m a.s.l. (Figure 5a and Table 5). SnowModel outputs were further used to calculate the annual cumulative runoff. The Jakobshavn runoff ranged from 1.81×10^9 m^3 y^{-1} (2001/02) to 5.21×10^9 m^3 y^{-1} (2004/05), indicating an average annual insignificant increase of 0.13×10^9 m^3 y^{-1} (R^2=0.13, $p<0.25$) for the simulation period (Figures 4 and 5d). The mean annual Jakobshavn runoff was $3.36(\pm1.1)\times10^9$ m^3 y^{-1} (equals 3.36 km^3 w.eq. y^{-1}), representing a specific runoff of 26.1(±5.5) l s^{-1} km^{-2} y^{-1} (Table 6). A specific Jakobshavn runoff

value which is approximately in the same order of magnitude with the value from the Kangerlussuaq drainage basin (67°N; 50°W) located 250 km to the south (for Kangerlussuaq the simulated runoff was validated against runoff observations). A Jakobshavn specific runoff almost 3.9 times the average specific runoff of 6.7(±1.0) l s^{-1} km^{-2} y^{-1} for the GrIS for the period 1995–2005 (Mernild et al. 2008).This indicates that the Jakobshavn runoff was above the spatial specific average runoff for the GrIS. For Jakobshavn, the ice discharge (calving) was estimated by Rignot et al. 2008 to be 52.6(±7.4) Gt y^{-1}, equals 47.3(±6.7) km^3 w.eq. y^{-1} (for the years 2000, 2004–2007). For both runoff and ice discharge the average trends are similar, indicating increasing (insignificant) influx of freshwater to the Illulissat Icefiord for the period 2000/01–2006/07 (Figure 5d). Based on the few common data points (2004–2007; n=4; Figure 5d), there is no reason statistically to conclude that: 1) the increasing runoff has any influence on the rapid increasing ice discharge, nor that; 2) an increasing flux of surface runoff in a warmer future climate will accelerate the volume of ice discharge. The understanding of the mechanisms that link changing climate to changing surface conditions, glacier hydrology, and ice sheet dynamics are still poorly understood.

The ice discharge was combined with the average SnowModel simulated surface runoff, to deduce the freshwater flux from the Jakobshavn drainage area (losses from geothermal heating/melting were omitted): a freshwater flux averaging around 50.7 km^3 y^{-1} to the Illulissat Icefjord. Around 3.4 km^3 y^{-1} (~7%) originated from the surface runoff, 47.3 km^3 y^{-1} (~93%) from ice discharge, for a total of ~51.0 km^3 y^{-1}. For the Jakobshavn drainage area runoff forms a minor part of the overall freshwater flux to the fiord, whereas e.g., further south at the Kangerlussuaq drainage area runoff accounts for 100% of the flux, due to the inland position of the GrIS margin.

To assist with calculating the net mass-balance conditions and the location of the ELA, the water balance (Equation 1) was divided into two different periods: 1) an accumulation period (September through May; winter period) where accumulation processes (precipitation and snow redistribution, influenced by blowing-snow sublimation) are dominant; and 2) an ablation period (June through August; summer period) where ablation processes (evaporation, sublimation, and melting) are dominant. Figure 6 illustrates the simulated net-mass balance variations for the Jakobshavn drainage area. The modeled ELA fluctuated from 990 to 1,210 m a.s.l, showing that Swiss Camp was positioned within the boundaries of the ELA-zone. JAR1 was positioned in the ablation area with a varying net mass-balance of -0.8 to -0.2 m w.eq. y^{-1}, and JAR2 and JAR3 with a varying net mass-balance between -2.4 to -1.1 m w.eq. y^{-1} and -3.5 to -1.7 m w.eq. y^{-1}, respectively. The location of the ELA is sensitive to changes in climate. The modeled ELA is in accordance with

observations; however Stober and Hepperle (2007) indicated that the ELA has moved to an elevation approximately 250 m higher than Swiss Camp by 2006. In general, in the 1990s Swiss Camp was located at the ELA, but the ELA moved to higher elevations during the beginning of this century due to increased melt in the area (Steffen et al. 2006).

6. Summary and conclusion

Quantifying freshwater runoff where observed datasets are available is relatively easily achieved, albeit possibly subject to significant uncertainties. This study presents simulations of the Jakobshavn surface melt extent and related water-balance components, focusing on surface runoff for the period 2000/01–2006/07. A robust, physically based, state-of-the-art snow and glacier-ice evolution modeling system (SnowModel) was used. Our SnowModel simulations have been validated against independent *in situ* observations (accumulation and ablation observations) made on the western GrIS: there is a high degree of agreement between these Jakobshavn simulations and the recorded observations. The simulated Jakobshavn series yielded useful insights into the present conditions of the ice sheet net mass-balance and the interannual runoff variability. The 2000/01–2006/07 mean annual surface runoff was ~3.4 $km^3\ y^{-1}$. In light of missing glacio-hydro-dynamic model routines, values from previous studies of the Jakobshavn ice discharge (52.6(±7.4) Gt y^{-1}, equals 47.3(±6.7) km^3 w.eq. y^{-1}), was adapted to provide estimates of the overall freshwater flux to the Illulissat Icefjord (~51.0 $km^3\ y^{-1}$). For both runoff and ice discharge the average trends are similar, indicating increasing (insignificant) influx of freshwater to the Illulissat Icefiord for the period 2000/01–2006/07. This study suggests that surface runoff forms a minor part of the overall freshwater flux to the fiord: ~7% (~3.4 $km^3\ y^{-1}$) of the average annual freshwater flux of ~51.0 $km^3\ y^{-1}$ originates from the surface runoff.

Acknowledgment

Special thanks to the Cooperative Institute for Research in the Environmental Sciences (CIRES), University of Colorado at Boulder, for the use of observed Swiss Camp snow water equivalent data, and for the use of meteorological data from stations related to the Greenland Climate Network (GC-Net). Further, special thanks to the Los Alamos National Laboratory (LANL) for the use of MODIS satellite images. Thanks to the Cooperative Institute for Research in the Atmosphere, Colorado State University, for hosting the first author during September and October 2008, and February 2009. This work was supported by grants from the University of Alaska

Presidential IPY Postdoctoral Foundation, and carried out during the first author's IPY Post Doc. Program at the UAF.

References

ACIA, 2005. Arctic Climate Impact Assessment. Cambridge University Press, 1042 p.

Allerup, P., H. Madsen, and F. Vejen, 1998. Estimating true precipitation in arctic areas. *Proc. Nordic Hydrological Conf.,* Helsinki, Finland, Nordic Hydrological Programme Rep. **44**: 1–9.

Allerup, P., H. Madsen, and F. Vejen, 2000. Correction of precipitation based on off-site weather information. *Atmos. Res.,* **53**: 231–250.

Bamber, J., S. Ekholm, and W. Krabill 2001. A new, high-resolution digital elevation model of Greenland fully validated with airborne laser altimeter data. *J. Geophys. Res.*, **106**(B4): 6733–6746.

Boggild, C. E., S. G. Warren, R. E. Brandt, and K. J. Brown 2006. Effects of dust and black carbon on albedo of the Greenland ablation zone. Abstract: American Geophysical Union, Fall Meeting 2006, abstract #U22A-05.

Broeke, M. van den, P. Smeets, J. Ettema, C. van der Veen, R. van de Wal, and J. Oerlemans 2008. partitioning of melt and meltwater fluxes in the ablation zone of the west Greenland ice sheet. *The Cryosphere*, **2**: 179–189.

Born, E. W., and J. Böcher, 2001. *The Ecology of Greenland.* Ministry of Environment and Natural Resources, Nuuk, Greenland, 429 pp.

Box, J. E., D. H. Bromwich, B. A. Vennhuis, L.-S. Bai, J. C. Stroeve, J. C. Rogers, K. Steffen, T. Haren, and S.-H. Wang, 2006. Greenland ice sheet surface mass balance variability (1988-2004) from calibrated Polar MM5 output. *Journal of Climate*, **19**: 2783–2800.

Chylek, P., M. McCabe, M. K. Dubey, and J. Dozier, 2007. Remote sensing of Greenland ice sheet using multispectral near-infrared and visible radiances. *Journal of Geophysical Research*, vol. **112**, D24S20, doi: 10.1029/2007JD008742.

Douville, H., J.-F. Royer, and J.-F. Mahfouf, 1995. A new snow paramerterization for the Meteo-France climate model. Part I: validation in stand-alone experiments. *Climate Dynamics*, **12**: 21–35.

Dowdeswell, J. A., J. O. Hagen, H. Björnsson, A. F. Glazovsky, W. D. Harrison, P. Holmlund, J. Jania, R. M. Koerner, B. Lefauconnier, C. S. L. Ommanney, and R. H. Thomas, 1997. The Mass balance of Circum-Arctic Glaciers and Recent Climate Change. *Quaternary Research*, **48**, 1–4, no. QR971900: 1–14.

Fettweis, X. 2007. Reconstruction of the 1979–2006 Greenland ice sheet surface mass balance using the regional climate model MAR. *The Cryosphere*, **1**: 21–40.

Hanna, E., P. Huybrechts, and T. Mote, 2002. Surface mass balance of the Greenland ice sheet from climate-analysis data and accumulation/runoff models. *Annals of Glaciology*, **35**: 67–72.

Hanna, E., P. Huybrechts, I. Janssens, J. Cappelen, K. Steffen, and A. Stephens, 2005. Runoff and mass balance of the Greenland ice sheet: 1958–2003. *J. Geophys. Res.*, **110**: 1–16.

Hanna, E., J. Box, and P. Huybrechts 2007. Greenland Ice Sheet mass balance. Arctic Report Card 2007, update to State of Arctic Report 2006, NOAA, available online at http://www.arctic.noaa.gov/reportcard/

Hanna, E., P. Huybrechts, K. Steffen, J. Cappelen, R. Huff., C. Shuman, T. Irvine-Fynn, S. Wise, and M. Griffiths, 2008. Increased Runoff from melt from the Greenland Ice Sheet: A response to Global Warming. *Journal of Climate*, **21**: 331–341.

Hanna, E., J. Cappelen, X. Fettweis, P. Huybrechts, A. Luckman, M. H. Ribergaard 2009. Hydrologic response of the Greenland Ice sheet: the role of oceanographic warming. *Hydrological Processes*, **23**: 7–30.

Holland, D. M., R. H. Thomas, B. de Young, M. H. Ribergaard, B. Lyberth, 2008. Acceleration of Jakobshavn Isbrae triggered by warm subsurface ocean waters. *Nature*, doi:10.1038/ngeo316: 659–664.

IPCC, 2007: Summary for Poicymakers. In: Climate Change 2007. The Physical Science Basis. Contribution of Working Group I to the Fourth Assessment Report of the Intergovernmental Panel on Climate Change [Solomon, S., D. Qin, M. Manning, Z. Chen, M. Marquis, K.B. Averyt, M.Tignor and H.L. Miller (eds.)]. Cambridge University Press, Cambridge, United Kingdom and New York, USA.

Janssens, I., and P. Huybrechts, 2000. The treatment of meltwater retention in mass-balance parameterisation of the Greenland Ice Sheet. *Ann. Glaciol.,* **31**: 133–140.

Johannessen, O. M., K. Khvorostovsky, M. W. Miles, and L. P. Bobylev, 2005. Recent ice sheet growth in the interior of Greenland, *Sciencexpress*, 1013–1016, doi:10.1126/science.1115356.

Joughin, I., I. M. Howat, M. Fahnestock, B. Smith, W. Krabill, R. B. Alley, H. Stern, and M. Truffer, 2008. Continued evolution of Jakobshavn Isbrae following its rapid speedup, *J. Geophys. Res.*, **113**, F04006, doi:10.1029/2008JF001023.

Krabill, W. E., and Coauthors, 2000. Greenland ice sheet: Highelevation balance and peripheral thinning. *Science,* **289**: 428–430.

Krabill W., E. Hanna, P. Huybrechts, W. Abdalati, J. Cappelen, B. Csatho, E. Frederick, S. Manizade, C. Martin, J. Sonntag, R. Swift, R. Thomas, and J. Yunge, 2004. Greenland Ice Sheet: Increased coastal thinning, *Geophys. Res. Lett.*, **31**, L24402, doi:10.1029/2004GL021533.

Lemke, P., J. Ren, R. B. Alley, I. Allison, J. Carrasco, G. Flato, Y. Fujii, G. Kaser, P. Mote, R. H. Thomas, and T. Zhang, 2007. Observations: Changes in Snow, Ice and Frozen Ground, in: Climate Change 2007: The Physical Science Basis, Contribution of Working Group I to the Fourth Assessment Report of the Intergovernmental Panel on Climate Change, edited by: Solomon, S., Qin, D., Manning, M., Chen, Z., Marquis, M., Averyt, K. B., Tignor M., and Miller, H. L., Cambridge University Press, United Kingdom and New York, USA.

Liston GE. 1995. Local Advection of Momentum, Heat, and Moisture during the Melt of Patchy Snow Covers. *Journal of Applied Meteorology*, **34**(7): 1705–1715.

Liston, G. E., and K. Elder, 2006a. A distributed snow-evolution modeling system (SnowModel). *Journal of Hydrometeorology*, **7**: 1259–1276.

Liston, G. E., and K. Elder, 2006b. A meteorological distribution system for high resolution terrestrial modeling (MicroMet). *Jounal of Hydrometeorology*, **7**: 217–234.

Liston, G. E., R. B. Haehnel, M. Sturm, C. A. Hiemstra, S. Berezovskaya, and R. D. Tabler, 2007. Simulating complex snow distributions in windy environments using SnowTran-3D. *Journal of Glaciology*, **53**: 241–256.

Liston GE, Hall DK. 1995. An energy-balance model of lake-ice evolution. *Journal of Glaciology* **41**: 373–382.

Liston, G. E., and C. A. Hiemstra, 2008: A simple data assimilation system for complex snow distributions (SnowAssim). *J. Hydrometeorology*, **9**: 989–1004.

Liston, G. E., C. A. Hiemstra, K. Elder, and D. W. Cline, 2008: Meso-cell study area (MSA) snow distributions for the Cold Land Processes Experiment (CLPX). *J. Hydrometeorology*, **9**: 957–976.

Liston, G. E., and M. Sturm, 1998. A snow-transport model for complex terrain. *J. Glaciol.* **44**: 498–516.

Liston, G. E., and M. Sturm, 2002. Winter Precipitation Patterns in Arctic Alaska Determined from a Blowing-Snow Model and Snow-Depth Observations. *Journal of Hydrometeorology*, **3**: 646–659.

Liston, G. E., J.-G. Winther, O. Bruland, H. Elvehøy, and K. Sand, 1999. Below surface ice melt on the coastal Antarctic ice sheet. *J. Glaciol.*, **45**(150): 273–285.

Luckman, A. and T. Murry, 2005. Seasonal variation in velocity before retreat of Jakobshavn Isbrae, Greenland. *Geophysical Research Letter*, vol **32**, L08501, doi:10.1029/2005GL022519.

Mernild, S. H. and G. E. Liston, 2009. The influence of air temperature inversion on snow melt and glacier surface mass-balance simulations, SW Ammassalik Island, SE Greenland. In review *Journal of Applied Meteorology and Climate*.

Mernild, S. H., G. E. Liston, and B. Hasholt, 2007. Snow-Distribution and Melt Modeling for Glaciers in Zackenberg River Drainage Basin, NE Greenland. *Hydrological Processes*. 21: 3249–3263. DOI: 10.1002/hyp.6500.

Mernild, S. H., G. E. Liston, B. Hasholt, and N. T. Knudsen, 2006. Snow distribution and melt modeling for Mittivakkat Glacier, Ammassalik Island, SE Greenland. *J. Hydrometeor.*, **7**: 808–824.

Mernild, S. H., G. E. Liston, C. A., Hiemstra, and K. Steffen, 2008. Surface Melt Area and Water Balance Modeling on the Greenland Ice Sheet 1995–2005. *J. Hydrometeor*, **9**(6): 1191–1211. doi: 10.1175/2008JHM957.1

Mernild, S. H., G. E. Liston, C. A. Hiemstra, and K. Steffen, 2009a. Record 2007 Greenland Ice Sheet surface melt-extent and runoff. *Eos Trans. AGU*, 90(2): 13–14.

Mernild, S. H., G. E. Liston, C. A. Hiemstra, K. Steffen, E. Hanna, and J. H. Christensen, 2009b. Greenland Ice Sheet surface mass-balance modeling and freshwater flux for 2007, and in a 1995–2007 perspective. *Hydrological Processes*, DOI: 10.1002/hyp.7354.

Nick, F. M, A. Vieli, I. M. Howat, and I. Joughin, 2009. Large-scale changes in Greenland outlet glacier dynamics triggred at the terminus. *Nature Geoscience*, **2**: 110–114.

Parizek, B. R. and Alley, R. B. 2004. Implications of increased Greenland surface melt under global-warming scenarios: Ice-sheet simulations, *Quat. Sci. Rev.* **23**: 1013–1027.

Pomeroy, J. W., and R. L. H. Essery, 1999. Turbulent fluxes during blowing snow: Field test of model sublimation predictions. *Hydrol. Processes,* **13**: 2963–2975.

Rignot, E., J. E. Box, E. Burgress, and E. Hanna 2008. Mass balance of the Greenland ice sheet from 1958 to 2007. *Geophysical research Letters*, vol. **35**, L20502, doi: 10.1029/2008GL035417.

Scambos, T. and T. Haran 2002. An image-enhanced DEM of the Greenland Ice Sheet. *Annals of Glaciology*, **34**: 291–298.

Steffen, K. 1995. Surface energy exchange during the onset of melt at the equilibrium line altitude of the Greenland ice sheet. *Annals of Glaciology*, **21**: 13–18.

Steffen, K. and J. Box, 2001. Surface climatology of the Greenland Ice Sheet: Greenland climate network 1995–1999. *Journal of Geophysical Research*, **106**(24): 33951–33964.

Steffen, K., J. H. Zwally, J. A. Rail, A. Behar, R. Huff. 2006. Climate Variability, Melt-Flow Acceleration, and Ice Quakes at the Western Slope of the Greenland Ice Sheet. American Geophysical Union, Fall Meeting 2006, abstract #U22A-01

Stober, M. and J. Hepperle, 2007. Changes in Ice Elevation and Ice Flow-Velocity in the Swiss Camp Area (West Greenland) between 1991 and 2006. *Polarforschung*, **76**(3): 109–118.

Strack, J. E., G. E. Liston, R. A. Pielke Sr. 2004. Modeling Snow Depth for Improved Simulation of Snow-Vegetation-Atmosphere Interactions. *Journal of Hydrometeorology*, **5**: 723–734.

Weidick, A. and O. Bennike, 2007. Quaternary glaciation history and glaciology of Jakobshavn Isbræ and the Disko Bugt region, West Greenland: a review. *Geol. Surv. Den. Green. Bull.* **14**, 78 pp.

Yang, D., S. Ishida, B. E. Goodison, and T. Gunther, 1999. Bias correction of precipitation data for Greenland. *Journal of Geophysical Research-Atmospheres*, **104**, (D6): 6171–6181.

Young, K. L., W. R. Bolton, A. Killingtveit, and D. Yang, 2006. Assessment of precipitation and snowcover in northern research basins. *Nordic Hydrol.* **37**(4–5) : 377–391.

Zwally, J. H., W. Abdalati, T. Herring, K. Larson, J. Saba, and K. Steffen, 2002. Surface melt-induced acceleration of Greenland ice-sheet flow. *Science*, **297**: 218–222.

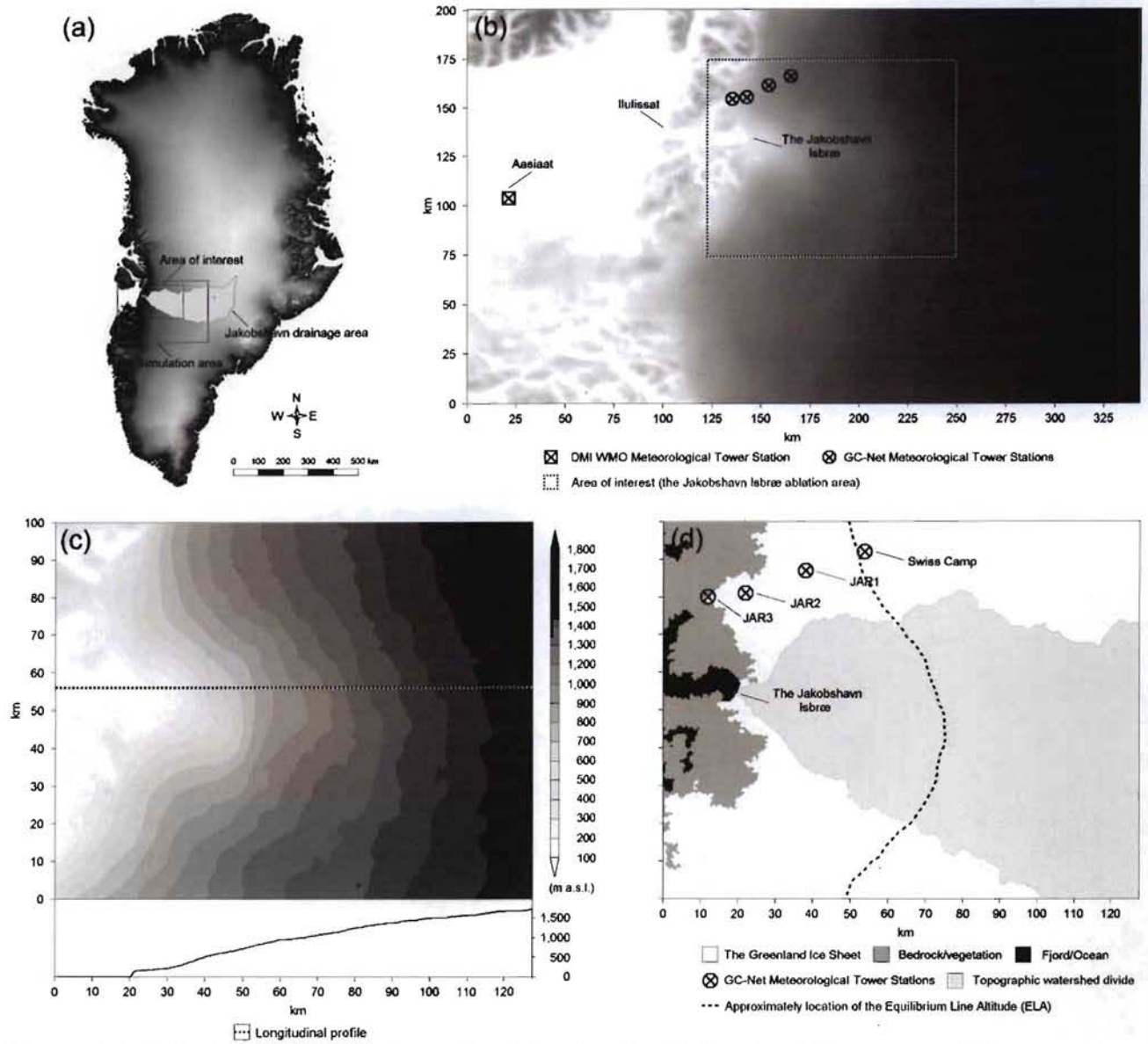

Figure 1: *(a) The Ilulissat region in western Greenland, with the simulation area and the area of interest, including the Jakobshavn Isbræ drainage area (5,340 km^2); (b) simulation area including meteorological tower stations; (c) area of interest with topography (gray shades, 100-m contour interval) and longitudinal profile; and (d) land cover characteristics in the area of interest including the four meteorological stations used for air temperature lapse rates: Swiss Camp (1,140 m a.s.l.), JAR1 (962 m a.s.l.), JAR2 (542 m a.s.l.), and JAR3 (283 m a.s.l.), the watershed divide, and the equilibrium line altitude (ELA).*

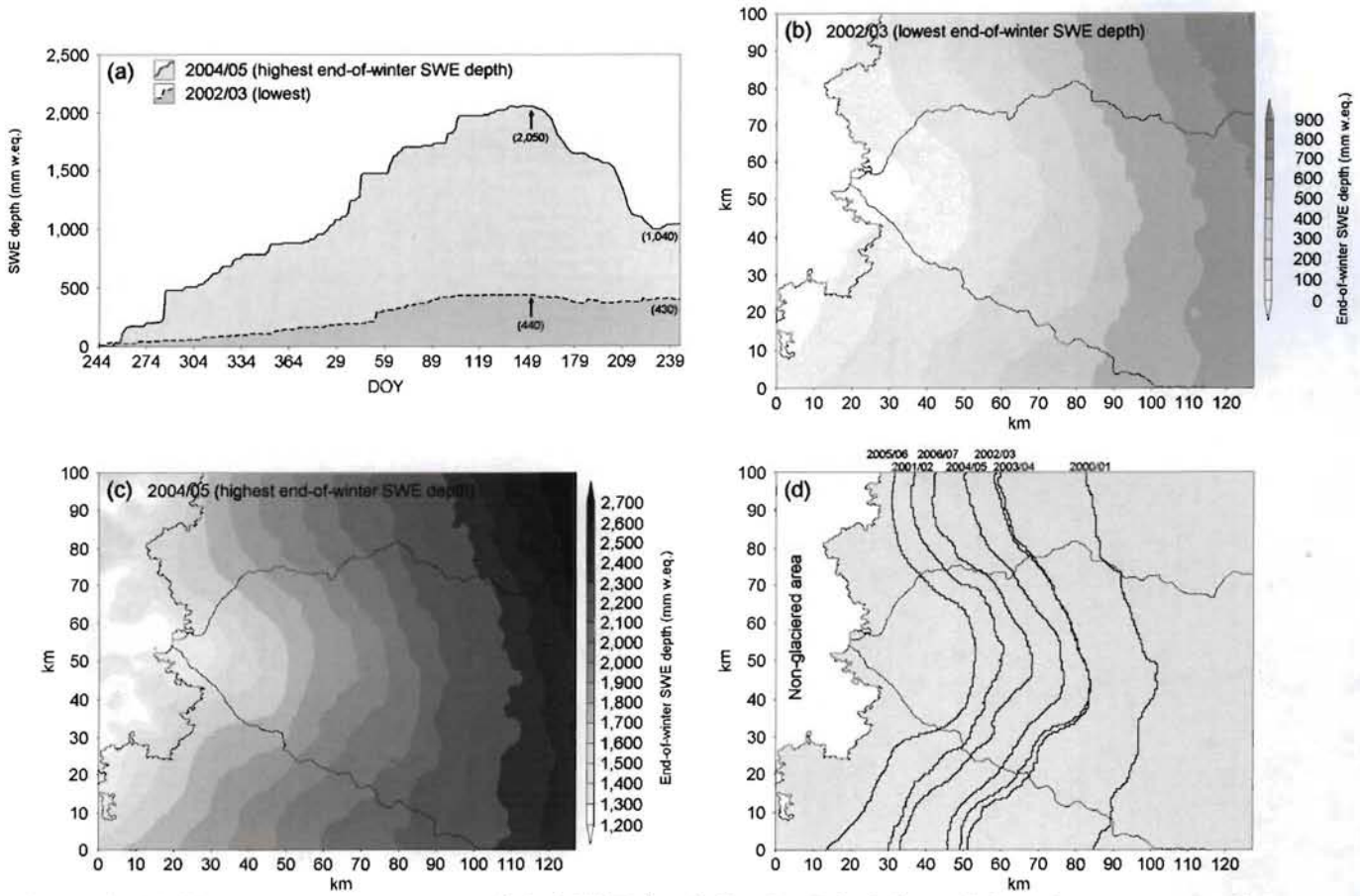

Figure 2: *(a) Variation in average modeled SWE depth for the Jakobshavn Isbræ drainage area for the year with the lowest (2002/03) and the highest (2004/05) average end-of-winter SWE depth. The numbers by the arrows indicate the average SWE depth on 31 May (end-of-winter period: accumulation period) and the other numbers the average SWE depth on 31 August (end-of-summer: ablation period); (b) spatial simulated SWE distribution for the end-of-winter (31 May 2003); (c) spatial simulated SWE distribution for the end-of-winter (31 May 2005); and (d) annual modeled maximum elevated snow line (the boundary between bare ice and snow cover on the glacier surface) from 2000/01 through 2006/07.*

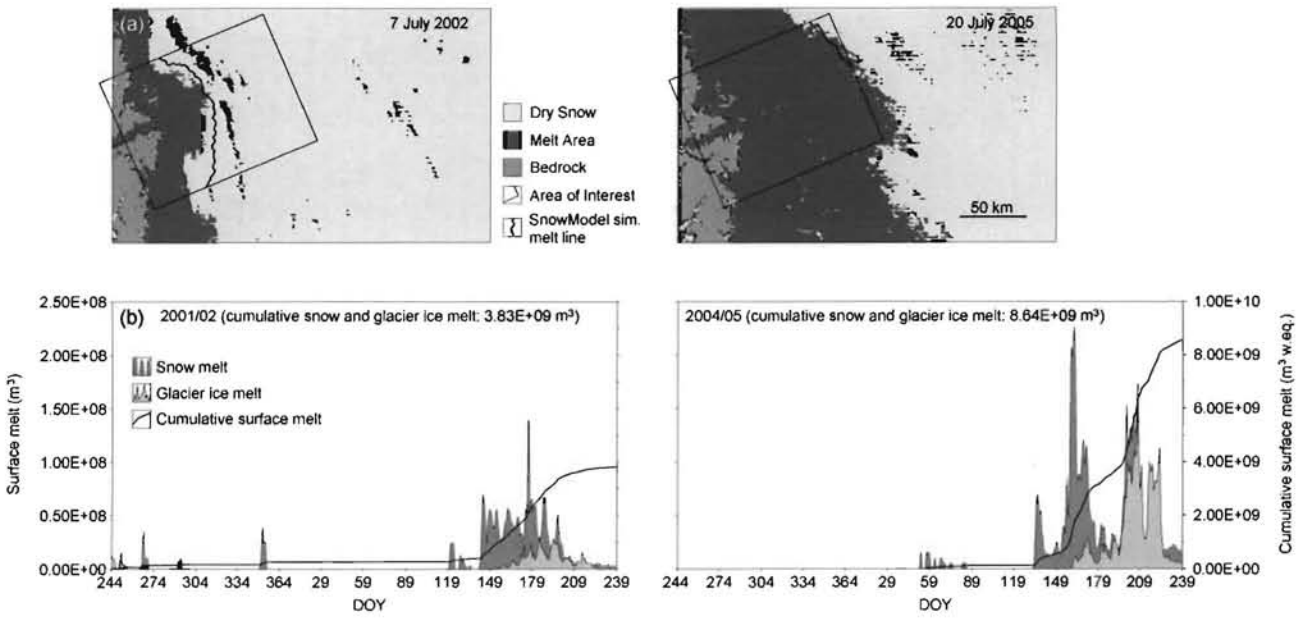

Figure 3: *(a) MODIS satellite-derived melt extent for 7 July 2002 (DOY 188) and 20 July 2005 (DOY 202) including SnowModel simulated line of melt extent for the Jakobshavn region; and (b) time series of daily modeled surface snow and glacier ice melt for the Jakobshavn Isbræ drainage area for 2001/02 (the year with the lowest annual cumulative surface melt) and 2004/05 (highest annual cumulative surface melt).*

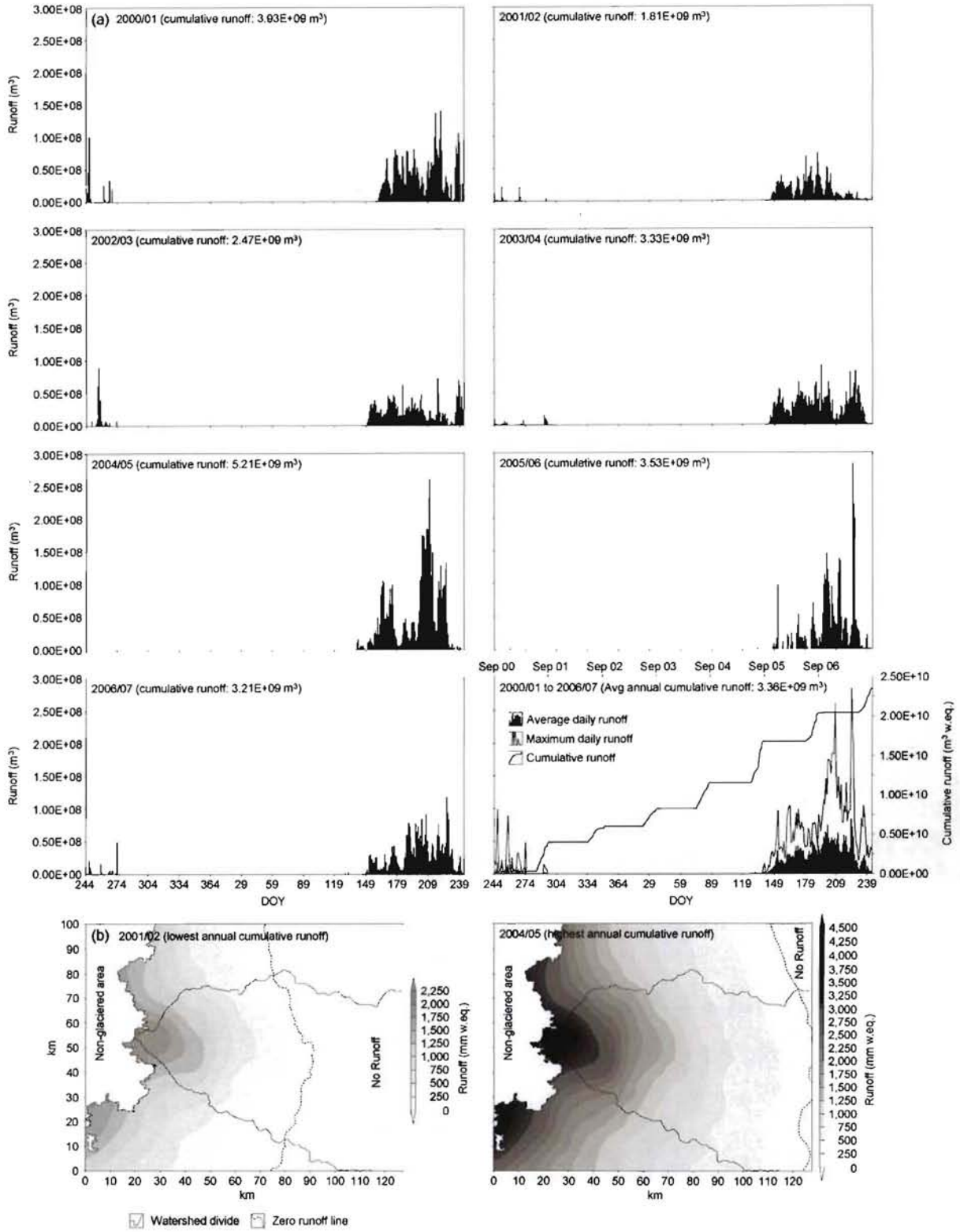

Figure 4: *(a) Time series of the daily modeled runoff for the Jakobshavn Isbræ drainage area from 2000/01 through 2006/07; and (b) spatial simulated runoff distribution for 2001/02 (the year with the lowest annual cumulative runoff) and 2004/05 (highest annual cumulative runoff).*

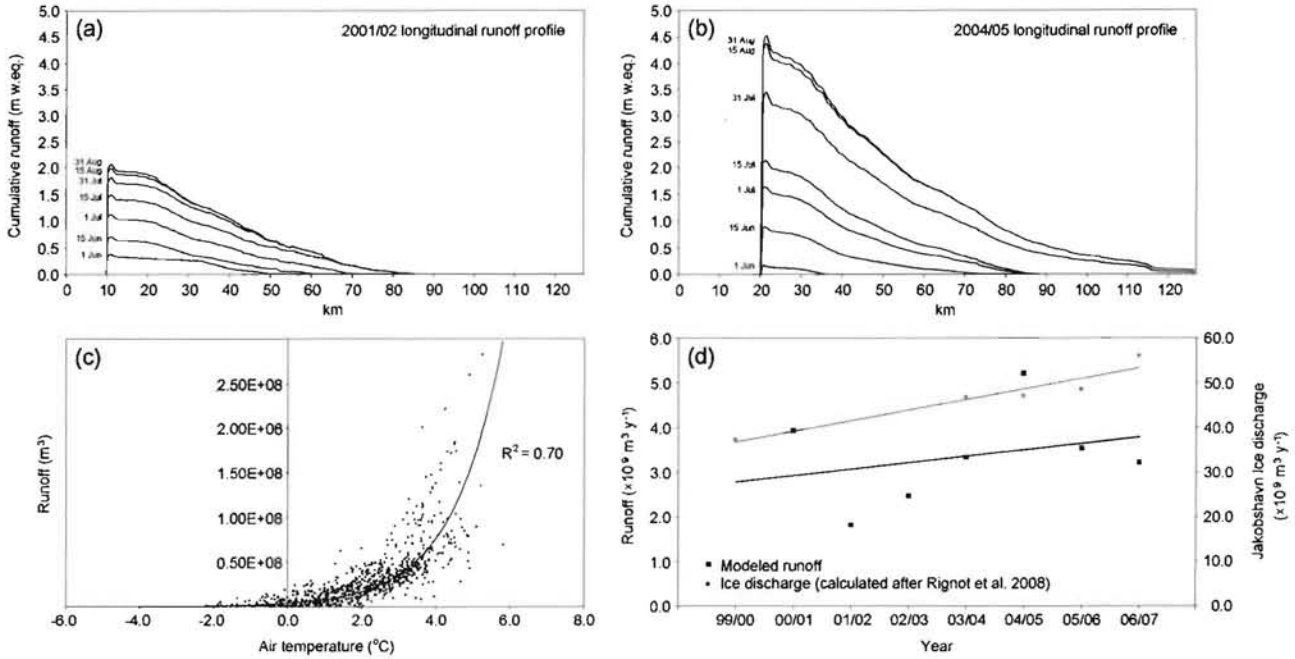

Figure 5: *(a and b) cumulative modeled longitudinal runoff profile for the year 2001/02 (the year with lowest annual runoff) and 2004/05 (highest annual runoff) calculated for every second week starting June 1 through August 31 (see longitudinal profile Figure 1c); (c) exponential relation between daily runoff and mean daily air temperature; and (d) time series for simulated annual runoff from 2000/01 through 2006/07 and Jakobshavn ice discharge from 2000, 2004 through 2007 based on data from Rignot et al. (2008).*

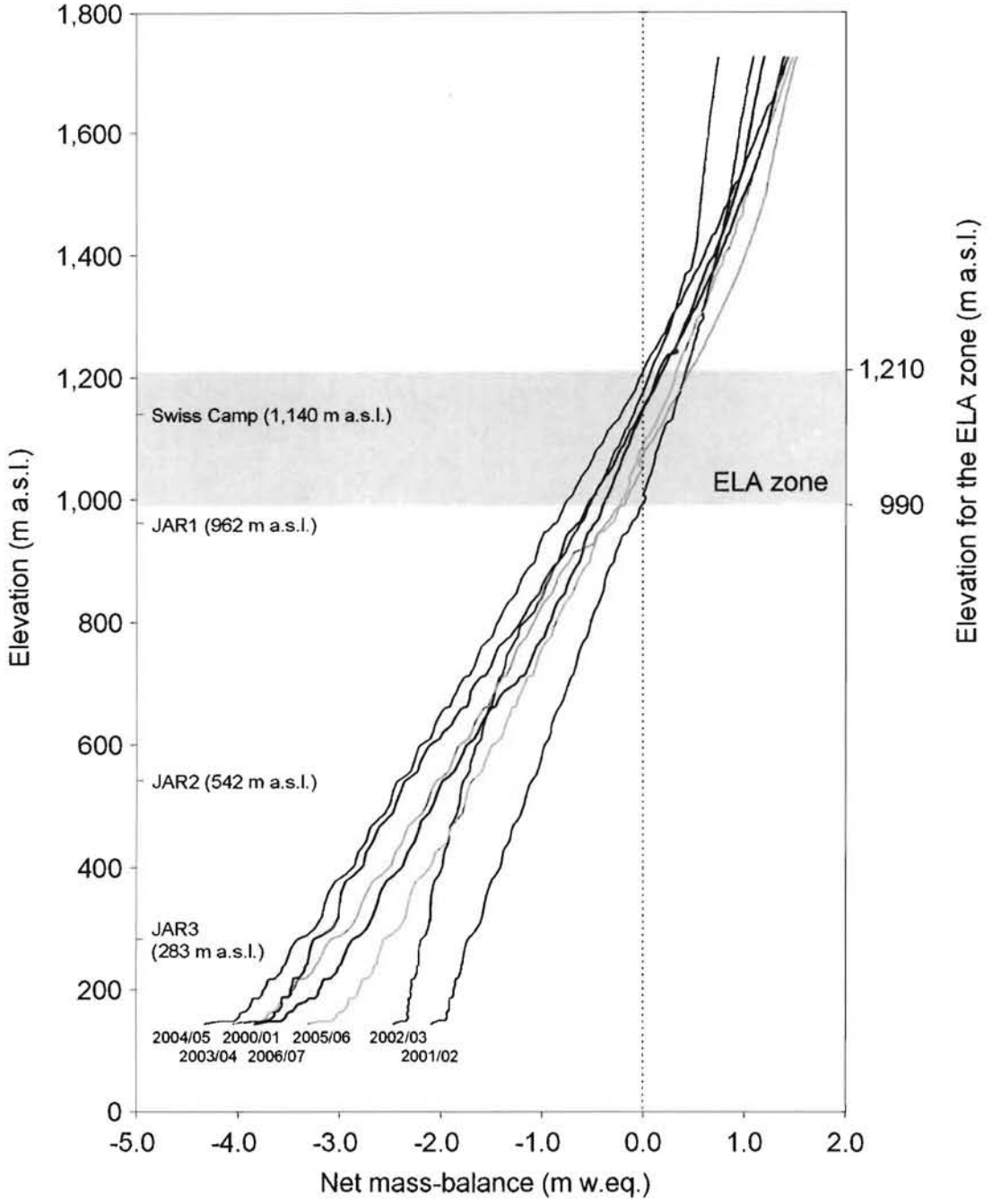

Figure 6: *Modeled net mass-balance in relation to elevation for the period 2000/01 through 2006/07 for the Jakobshavn Isbræ drainage area.*

Table 1: *User-defined constants used in the SnowModel simulations (see Liston and Sturm (1998) for parameter definitions).*

Symbol	Value	Parameter
C_v		Vegetation snow-holding depth (equal surface roughness length) (m)
	0.50	- Barren bedrock/vegetation
	0.01	- Lake/fiord/ocean (only when it is frozen)
	0.01	- Ice/snow
F	500.0	Snow equilibrium fetch distance (m)
U_{*t}	0.25	Threshold wind-shear velocity (m s^{-1})
Z_0	0.01	Snow surface roughness length (m)
dt	1	Time step (day)
$dx = dy$		Grid cell increment (km)
	0.5	- Jakobshavn simulation area
α		Surface albedo
	0.5–0.8	- Snow (variable snow albedo according to surface snow characteristics)
	0.4	- Ice
ρ		Surface density (kg m^{-3})
	280	- Snow
	910	- Ice
ρ_s	550	Saturated snow density (kg m^{-3})

***Table 2**: Mean monthly air temperature lapse rates for the Jakobshavn area based on data from the transect between the meteorological stations: JAR1 (962 m a.s.l.), JAR2 (542 m a.s.l.), and JAR3 (283 m a.s.l.) (from 1997 through 2005). See Figure 1b for meteorological station locations. For the GrIS the mean monthly lapse rates are based on temperature data from the Greenland coastal areas and the GrIS (from 1997 through 2005) (for further info see Mernild et al. 2008a).*

	Jan	Feb	Mar	Apr	May	Jun	Jul	Aug	Sep	Oct	Nov	Dec	Avg
Jakobshavn Icebrae area, °C km^{-1}	-7.7	-8.1	-7.3	-5.2	-6.6	-4.5	-4.7	-5.8	-8.7	-10.0	-7.5	-7.9	-7.1
Average GrIS (Mernild et al. 2008)	-7.8	-8.3	-7.8	-7.0	-6.7	-5.8	-6.9	-6.4	-7.7	-8.6	-8.7	-7.9	-7.5

***Table 3:** Meteorological input data for the Jakobshavn SnowModel simulations. Meteorological station data on the GrIS (Swiss Camp, JAR1 through JAR3) were provided by the Greenland Climate Network (GC-Net) from the Steffen Research Group at CIRES, and coastal meteorological station data (Aasiaat) by the Danish Meteorological Institute (DMI).*

Meteorological station name	Location	Data time period	Altitude (m a.s.l.)
Swiss Camp	69°34′03″N, 49°19′17″W	1 Sep 2000–9 May 2006	1,140
JAR1	69°29′51″N, 49°41′16″W	25 May 2001–31 Aug 2007	962
JAR2	69°25′09″N, 50°03′55″W	1 Sep 2000–31 Aug 2007	542
JAR3	69°23′40″N, 50°18′36″W	1 Jan 2001–24 May 2004	283
Aasiaat	68°42′00″N, 52°45′00″W	1 Sep 2000–31 Aug 2007	88

Table 4: *Observed and modeled SWE depth for the Swiss Camp and for the lower ablation zone of the Jakobshavn Isbræ drainage area at the beginning of May (10 May) and the end-of-winter (31 May) (for area specifications see Figure 1d).*

Year	Observed average SWE depth at the Swiss Camp carried out at the beginning of May (mm w.eq.)	Modeled SWE depth at the beginning of May (10 May) at the Swiss Camp based on precipitation data from the meteorological stations (mm w.eq.)	Modeled SWE depth at the beginning of May (10 May) at the Swiss Camp, based on iterative precipitation adjustment routines described in Mernild et al (2006a) and Liston and Hiemstra (2008) (mm w.eq.)	Maximum, average, and minimum modeled SWE depth at the beginning of May (10 May) for the Jakobshavn Isbræ drainage area (mm w.eq.)	Maximum, average, and minimum modeled end-of-winter (31 May) SWE depth for the Jakobshavn Isbræ drainage area (mm w.eq.)
2000/01	1,200	990	1,190	1,930 1,330±310 660	2,050 1,410±330 690
2001/02	1,220	1,360	1,210	1,840 1,340±260 530	1,840 1,330±270 530
2002/03	330	410	330	820 440±200 40	820 440±190 1
2003/04	1,440	1,010	1,450	2,260 1,600±340 820	2,300 1,610±370 510
2004/05	1,860	1,320	1,850	2,690 2,020±350 1,290	2,740 2,050±350 1,130
2005/06	1,310	990	1,300	2,120 1,470±330 760	2,210 1,520±340 720
2006/07	1,070	1,240	1,080	1,710 1,190±270 590	1,790 1,240±290 530
Average and standard deviation	1,200±460	1,045±320	1,200±460	1,910±580 1,340±480 670±370	1,960±600 1,370±490 590±340

Table 5: *Mean temperature and positive degree day for June through August, maximum modeled snow line elevation, melt elevation, and runoff elevation, and day of year (DOY) for the first day of summer runoff and for the runoff period.*

	2000/01	2001/02	2002/03	2003/04	2004/05	2005/06	2006/07	Average and /or standard deviation
Mean temperature (°C) and positive degree day for June, July, and August	2.7 258	1.7 173	1.7 169	2.5 233	1.9 188	0.9 128	2.4 219	2.0±0.6 195±44
Maximum and average maximum modeled snow line (m a.s.l.)	1,413 1,397±11	1,005 928±26	1.243 1,213±16	1,251 1,236±10	1,158 1,145±5	963 939±9	1,027 1,014±5	974±457 1,125±173
Maximum and average maximum modeled elevation for runoff (m a.s.l.)	1,666 1,606±3	1,482 1,477±3	1,431 1,418±6	1,498 1,493±3	1,879 1,868±5	1,804 1,795±3	1,541 1,538±2	1,614 1,599±170
First day of modeled summer runoff, DOY	159	138	150	143	139	133	129	142±10
Number of days with modeled runoff	96	114	109	123	99	86	115	97±17
Continuously modeled runoff period during summer, DOY	162–233	145–244	150–229	143–240	150–234	186–242	149–243	155–238

Table 6: *Modeled specific runoff (Rs) for the lower ablation zone of the Jakobshavn Isbræ drainage area from 2000/01 through 2006/07. The runoff values do not include hydroglacio processes such as the sudden release of bulk water.*

	2000/01	2001/02	2002/03	2003/04	2004/05	2005/06	2006/07	Average and standard deviation
Specific modeled runoff (Rs; $l\ s^{-1}\ km^{-2}$)	30.3	17.7	26.7	31.9	28.8	19.3	28.1	26.1±5.5